Protein Science (2000), *9*:1889–1897. Cambridge University Press. Printed in the USA.

Structure of a rat α_1-macroglobulin receptor-binding domain dimer

TSAN XIAO,[1] DIANNE L. DECAMP,[2] AND STEPHEN R. SPRANG[1,3]

[1]Department of Biochemistry, The University of Texas Southwestern Medical Center, 5323 Harry Hines Boulevard, Dallas, Texas 75390
[2]Department of Pharmacology, The University of Texas Southwestern Medical Center, 5323 Harry Hines Boulevard, Dallas, Texas 75390
[3]Howard Hughes Medical Institute, The University of Texas Southwestern Medical Center, 5323 Harry Hines Boulevard, Dallas, Texas 75390

(RECEIVED May 17, 2000; FINAL REVISION July 20, 2000; ACCEPTED July 24, 2000)

Abstract

α-Macroglobulin inhibits a broad spectrum of proteinases by forming macromolecular cages inside which proteinases are cross-linked and trapped. Upon formation of a complex with proteinase, α-macroglobulin undergoes a large conformational change that results in the exposure of its receptor-binding domain (RBD). Engagement of this domain by α-macroglobulin receptor permits clearance of the α-macroglobulin: proteinase complex from circulation. The crystal structure of rat α_1-macroglobulin RBD has been determined at 2.3 Å resolution. The RBD is composed of a nine-stranded β-sandwich and a single α-helix that has been implicated as part of the receptor binding site and that lies on the surface of the β-sandwich. The crystallographic asymmetric unit contains a dimer of RBDs related by approximate twofold symmetry such that the putative receptor recognition sites of the two monomers are contiguous. By gel filtration and ultracentrifugation, it is shown that RBD dimers form in solution with a dissociation constant of ~50 μM. The structure of the RBD dimer might mimic a conformation of transformed α-macroglobulin in which the proposed receptor binding residues are exposed on one face of the dimer. A pair of phenylalanine residues replaces a cystine that is conserved in other members of the macroglobulin family. These residues participate in a network of aromatic side-chain interactions that appears to stabilize the dimer interface.

Keywords: α_1 macroglobulin; quaternary structure; receptor-binding domain; X-ray crystallography

Alpha macroglobulins (αMs) constitute a family of large glycoproteins that inhibit all four types of proteinases by a trapping mechanism (Sottrup-Jensen, 1989). Most members of this family of 180 kD proteins form tetrameric complexes under physiological conditions, although some exist as functional monomers or dimers, especially in phylogenetically ancient species (Sottrup-Jensen, 1987). Each member contains three characteristic sequence motifs: a bait region that is cleaved by target proteinases (residues 667 to 705 in human α_2M), a cysteine-glutamate pair that forms a reactive thiol ester, and a carboxyl-terminal ~140 residue domain that binds the αM receptor/low-density lipoprotein receptor-related protein (LRP). After cleavage by proteinase at the bait region, αM undergoes a conformational change that increases the reactivity of the intrachain thioester, leading to the formation of an ϵ-Lys (proteinase)-γ-Glu952 (αM) cross-link at the thiol ester site. Formation of this so-called "transformed" species leads to entrapment of the proteinase within the large cavity of the αM tetramer and renders it inaccessible to its substrates. This conformational change also exposes the C-terminal receptor binding sites in the receptor binding domain (RBD). High affinity binding of αM to LRP results in clearance of αM: proteinase complexes from circulation. Exposure of RBD can also be induced by incubating αM with methylamine, which directly attacks the thiol ester bonds but leaves the bait region intact (Swenson & Howard, 1979). Proteinase or methylamine-induced transformation of αM increases its electrophoretic mobility, generating the so-called "fast" form of αM (Sottrup-Jensen, 1987). In addition to its function as a proteinase inhibitor, αM also binds several hormones, growth factors, and β-amyloid peptide (O'Connor-McCourt & Wakefield, 1987; Borth & Luger, 1989; Hughes et al., 1998). This has evoked the proposal that αM may regulate immune responses, participate in tissue remodeling and be involved in neuropathologenic pathways leading to Alzheimer's disease (Sottrup-Jensen, 1989; Woessner, 1991; Blacker et al., 1998; Armstrong & Quigley, 1999).

LRP, a member of the low-density lipoprotein (LDL) receptor family, is a multifunctional receptor that binds various ligands such as receptor associated protein (RAP), lipoprotein lipase and lipo-

Reprint requests to: Stephen R. Sprang, Howard Hughes Medical Institute, Department of Biochemistry, University of Texas Southwestern Medical Center, 5323 Harry Hines Boulevard, Dallas, Texas 75390-9050; e-mail: sprang@chop.swmed.edu.

proteins, in addition to αM (Gliemann et al., 1994). α_2M binds to two clusters of repeats on LRP, known as clusters II and IV; within the former, a series of five complement repeats are essential for binding (Neels et al., 1999). Calcium specifically binds LRP at several sites to induce a receptor conformation that is competent for ligand recognition (Moestrup et al., 1990). Structures of ligand binding repeats from LDL receptor (Fass et al., 1997) and the receptor binding domain of apolipoprotein E (Wilson et al., 1991) suggest that the interaction between LRP and apolipoprotein E could be mediated by electrostatic contacts between negatively charged receptor residues and positively charged ligand residues. Human α_2M binds to cross-linked receptors with greater affinity ($K_d \sim 40$ pM) than to monomeric LRP ($K_d \sim 2$ nM), indicating that α_2M tetramers are able to bind at least two receptor molecules simultaneously (Moestrup & Gliemann, 1991). The RBD fragment of human α_2M, which can be released by proteolysis after treatment with methylamine, has a much lower affinity ($K_d = 60$–125 nM) for LRP than intact α_2M (Sottrup-Jensen et al., 1986). Inclusion of the 15 α_2M residues amino-terminal to the RBD affords a 5- to 10-fold increase in its affinity for LRP, indicating that bordering residues may affect receptor affinity either by modulating RBD conformation or providing additional binding surface (Holtet et al., 1994; Nielsen et al., 1995).

Three αM orthologs are expressed in rat: α_1M (tetramer), α_2M (tetramer), and α_1 inhibitor 3 monomer ($\alpha_1 I_3$) (Eggertsen et al., 1991; Warmegard et al., 1992). In contrast to the other two proteins, rat α_1M is present in most tissues and is expressed constitutively in plasma. In this regard, rat α_1M appears to function as a "housekeeping" macroglobulin while the other two are acute phase proteins. Human α_2M is not an acute phase protein and performs functions equivalent to those of rat α_1M. Cryo-electron microscopy studies of native and transformed human α_2M using monoclonal antibodies yield projection images of the tetramer in which RBD appears to be positioned at the tip of the molecule (Delain et al., 1988; Stoops et al., 1994). The 10 Å crystal structure of transformed human α_2M tetramer has the appearance of a large sphere to which four symmetry-related domains, postulated to be the RBD, are loosely attached (Andersen et al., 1995). Studies of bovine and human α_2M RBD structures by X-ray crystallography and NMR spectroscopy, respectively, reveal an overall β-sandwich fold. The receptor recognition site consists of the β_4-α-β_5 motif (Jenner et al., 1998; Huang et al., 2000). In addition, a calcium binding site was identified in the structure of bovine RBD (Jenner et al., 1998).

Here, we present the crystal structure of the rat α_1M receptor-binding domain. The crystallographic asymmetric unit consists of a pseudo-symmetric dimer of RBD with the proposed receptor binding residues exposed on one surface of the dimer. The quaternary structure observed in the crystals appears to be a direct consequence of RBD dimerization in solution and may provide insights into the mechanism by which RBD binds receptors in vivo.

Results and discussion

Crystallization and structure determination

Rat α_1M RBD was expressed as an N-terminal hexa-histidine tagged recombinant fusion protein in *Escherichia coli*. The expressed protein is readily soluble and amenable to purification. By size exclusion chromatography and equilibrium ultracentrifugation, we demonstrated that α_1M RBD forms multimers, primarily dimers, in solution (Fig. 1). Dimers form spontaneously from purified monomers within 12 h.

Crystals of rat α_1M RBD are needle-shaped and belong to space group $P2_1$ with two molecules in the asymmetric unit. Removal of dimers by gel filtration and the use of alternative precipitants and salts do not affect crystal morphology. Fresh crystals doubled in thickness after macroseeding, at the expense of an increase in mosaicity. Diffraction data were measured from cryoprotected crystals to a resolution of 2.3 Å using the F1 beamline at the Cornell High Energy Synchrotron Source.

The structure was solved by the method of molecular replacement using the coordinates of bovine α_2M RBD (Jenner et al., 1998) as a search model. The asymmetric unit contains two molecules of RBD (designated RBDa and RBDb; residue suffixes "a" and "b" refer to residues in molecules RBDa and RBDb, respectively) related by approximate twofold symmetry (Fig. 2). The model has been refined to $R_{work} = 0.228$ and $R_{free} = 0.264$ and includes residues 3–136 of RBDa and residues 3–132 of RBDb (residue 1 corresponds to the start of RBD at rat α_1M residue 1336 and human α_2M residue 1313), together with 94 ordered water molecules (Table 1). The major structural differences between rat α_1M RBD and bovine α_2M RBD are confined to segments that connect the β-strands, as discussed below.

Comparison with bovine and human structures

Like bovine and human α_2M RBD, rat α_1M RBD forms a nine-stranded β-sandwich with a single helix inserted in the loop between β4 and β5 (Fig. 2). β-strands 1, 2, 7 and 4 make up one sheet and 5, 6, 3, 8, and 9 the other. Using the nine β-strands and single conserved helix (henceforth referred to as the "core") to superimpose the bovine and rat structures, the root-mean-square displacement (RMSD) for 67 Cα pairs is 0.38 and 0.46 Å for RBDa and RBDb, respectively. The β1–β2 loop (residues 15–24) is the locus of the largest conformational differences between the structures of bovine and rat RBD: the main chains of the two molecules in this region are displaced by more than 10 Å from each other after superposition of their core domains (Fig. 3A). The β1–β2 loops mediate dimer formation between the two molecules in the asymmetric unit, whereas the corresponding residues in the bovine and human homologs are folded into short helices (Jenner et al., 1998; Huang et al., 2000) (Fig. 3A). In part, these differences may be a consequence of the substitution of the disulfide bridge between C17 and C132 in human RBD (C17 and C131 in bovine RBD) by a pair of phenylalanine residues in rat RBD (Fig. 3B). The β7–β8 loop also participates in dimer formation and its conformation differs from that observed in the structures of human and bovine RBD.

Binding of αM to LRP is Ca^{2+}-dependent (Herz et al., 1988; Moestrup et al., 1990). The β8–β9 loop of bovine RBD binds a calcium ion that is coordinated by the side chains of E121 and N76 (from a crystallographically related molecule), the main-chain carbonyl of D120 and four water molecules. The nearby D120 and E126 side chains are not involved in Ca^{2+} binding (Jenner et al., 1998) (Fig. 3A). In contrast, no electron density is present near the corresponding site of rat RBD, despite the presence of 25 mM calcium chloride in the crystallization buffer. Differences in the conformation of the β8–β9 loop among the structures of the three RBD homologs indicate that it is inherently flexible, despite high sequence conservation in this segment among RBD homologs

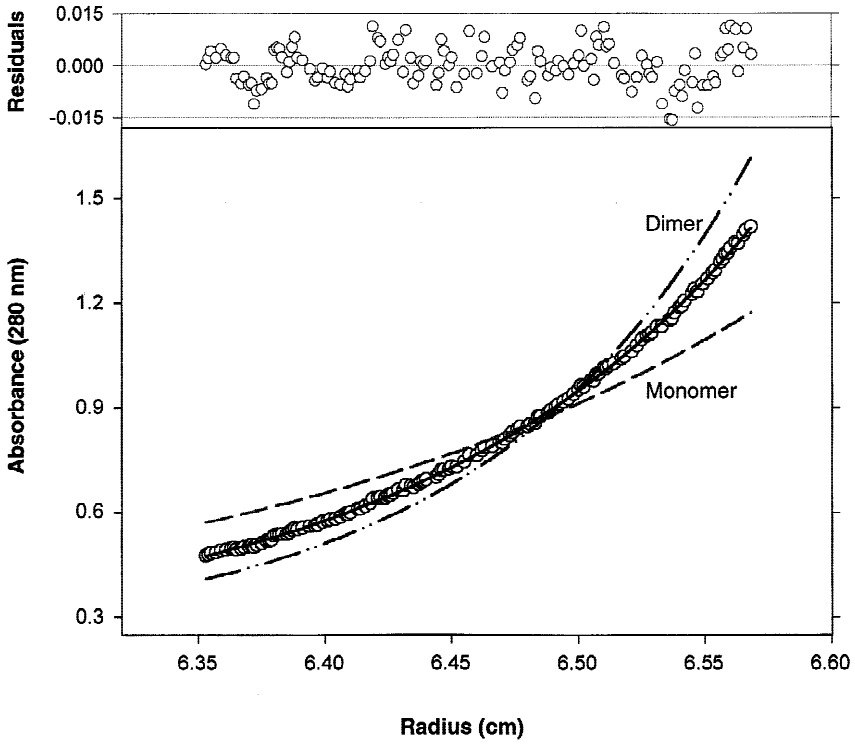

Fig. 1. Sedimentation equilibrium analysis of rat α_1M RBD. The circles and solid line represent the experimental data obtained at 4 °C, 18,000 rpm and the best fit of the former with the residuals displayed in the top panel. The dashed and dash-dot lines represent the predicted monomer and dimer profiles, respectively. Data analysis was performed with MicroCal Origin program version 4.1.

(Fig. 3B). In light of the substantial involvement of water in the coordination sphere of Ca^{2+} in bovine RBD and its absence in the rat structure, we suggest that RBD is not the major locus of Ca^{2+} binding. Structural studies of complement repeat units of LRP reveal a conserved Ca^{2+} binding site that might stabilize the binding domain and therefore account for the Ca^{2+}-dependence of LRP binding to αM (Moestrup et al., 1990; Huang et al., 1999; Dolmer et al., 2000).

Visual inspection of the human RBD structure indicates that the two β-sheets are packed more closely together than those of bovine and rat structures (Huang et al., 2000). Differences between the solution structure of human RBD and its bovine and rat ho-

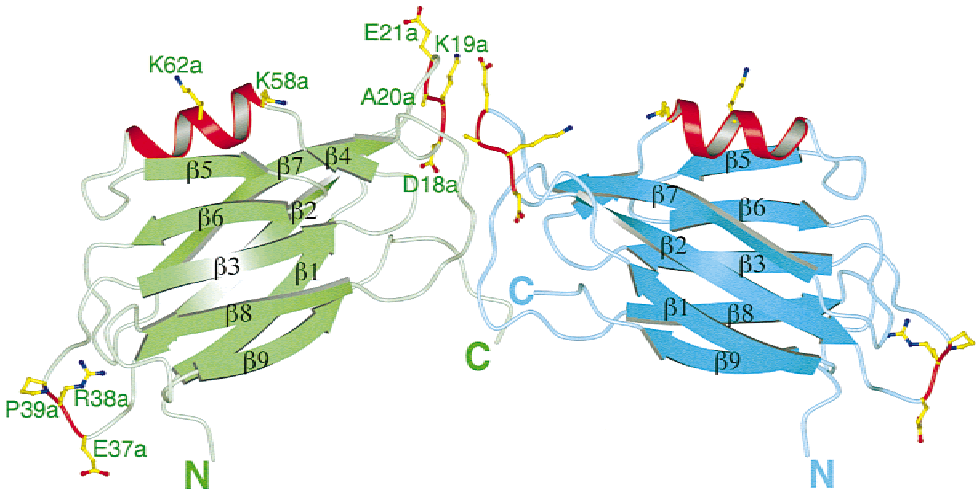

Fig. 2. The crystallographic asymmetric unit comprising a dimer of rat α_1MRBD. RBDa is colored green and RBDb, cyan. The three putative receptor binding segments (see text) are colored red and residues in these segments are displayed as ball-and-stick models.

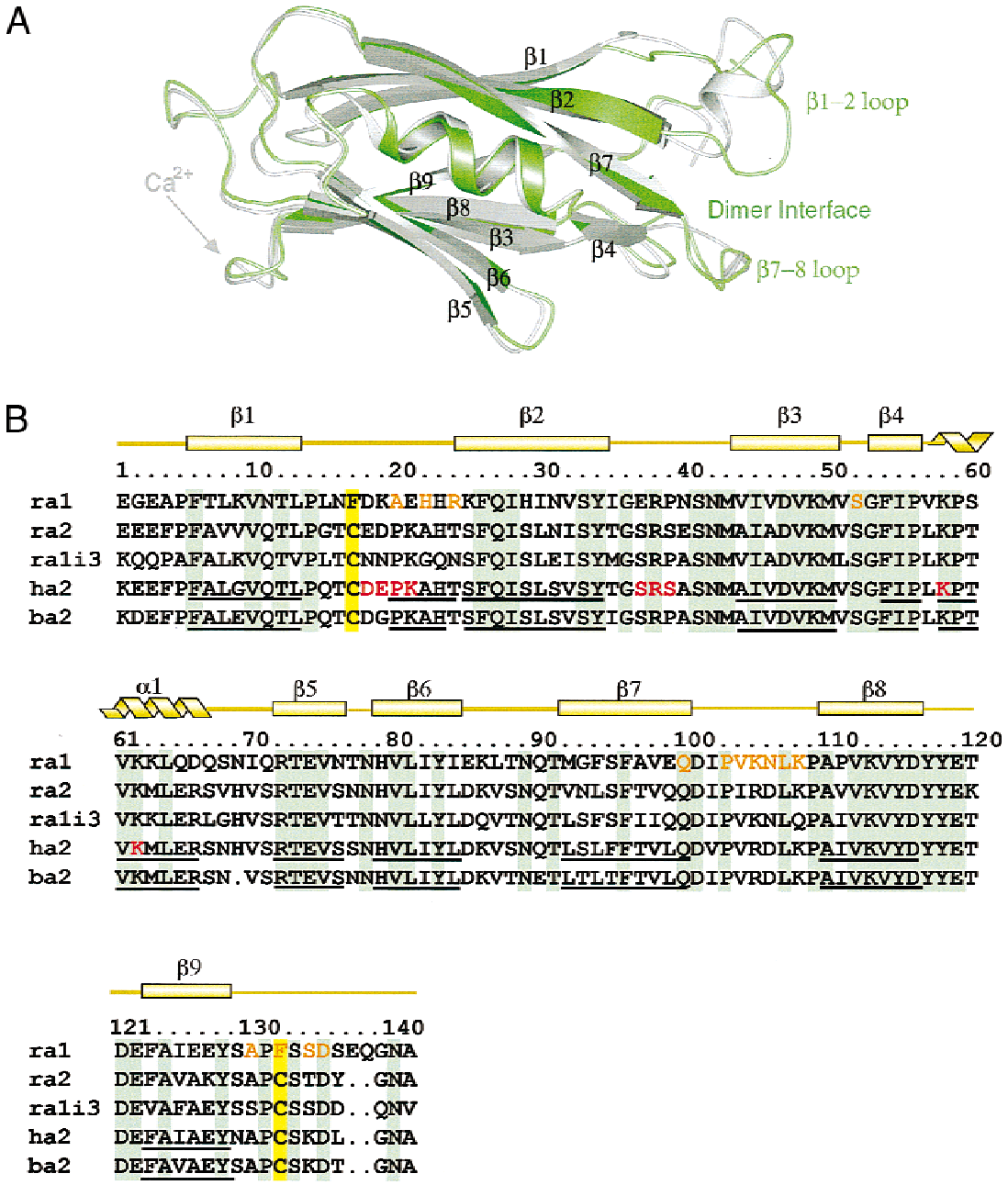

Fig. 3. Structural and sequence comparison of RBD homologs. **A:** Superposition of rat α_1M and bovine α_2M RBD structures with bovine RBD colored gray; the dimer is rotated approximately 90° about the horizontal relative to the view shown in Figure 2. The calcium binding site in the structure of bovine α_2M and the structural elements at the dimer interface in the structure of rat α_1M are indicated. **B**: Amino acid sequence alignment of the receptor binding domains from rat α_1-macroglobulin (ra1), rat α_2-macroglobulin (ra2), rat α_1 inhibitor III (ra1i3), human α_2-macroglobulin (ha2), and bovine α_2-macroglobulin (ba2). Residue 1 corresponds to ra1 residue 1336 or ha2 residue 1313. Because bovine RBD has a one-residue deletion in the loop at the N-terminal of β5, its residue numbering is different from other RBDs for the C-terminal half. The secondary structures of ra1 are displayed over the sequences, whereas those of ha2 and ba2 are marked as underlined residues. Strictly conserved residues are shaded in green. Residues involved in disulfide bonds or stabilizing the aromatic side-chain packing (see text) are displayed in yellow shade. Proposed receptor binding residues on ha2 are displayed in red letters. Dimer interface residues of ra1 are displayed in orange letters.

mologs (approximately 1.7 Å for the 67 core Cα pairs) are considerably larger than those between the latter two, even though the amino acid sequence of rat RBD shows equal similarity to both (63% sequence identity vs. 60%). Further discussion focuses on structures of bovine and rat RBDs.

Pseudo-symmetric dimers in the asymmetric unit

The asymmetric unit contains two molecules of RBD related by a rotation of about 179.2° and a translation of 2.9 Å (Fig. 2). The β1–β2 and β7–β8 loops of the two monomers interlace to form a

Table 1. *Summary of data collection and refinement statistics*

Data collection	
Resolution range (Å)	15.0–2.3
Space group	$P2_1$
Unit cell (Å)	a = 64.38, b = 36.15, c = 77.98, β = 105.9°
Reflections (total/unique)	48,604/14,814
$\langle I\rangle/\langle\sigma_I\rangle$	19.5 (3.8)[a]
Completeness (%)	94.6 (72.5)
R_{merge} (%)[b]	6.5 (20.5)
Model refinement	
Number of protein atoms	2,142
Number of water atoms	94
RMSD bond lengths (Å)	0.006
RMSD bond angles (deg)	1.278
RMSD bonded B-factors (Å^2)	1.862 (2.766)[c]
R_{work} (%)[d]	22.8
R_{free} (%)[e]	26.4
Average B-factor (Å^2)	46.1
Ramachandran plot	88.6% core, 11.4% allowed

[a] Numbers in parentheses correspond to the last resolution shell.
[b] $R_{merge} = \sum_h\sum_i|I_i(h) - \langle I(h)\rangle|/\sum_h\sum I_i(h)$, where $I_i(h)$ and $\langle I(h)\rangle$ are the i^{th} and mean measurement of the intensity of reflection h.
[c] Bonded main-chain (side-chain) B-factors.
[d] $R_{work} = \sum_h||F_{obs}(h)| - |F_{calc}(h)||/\sum_h|F_{obs}(h)|$, where $F_{obs}(h)$ and $F_{calc}(h)$ are the observed and calculated structure factors, respectively.
[e] Ten percent of the complete data set was excluded from refinement to calculate R_{free}.

dimer that buries 1,250 Å^2 of solvent accessible surface (Figs. 2, 4). The C-termini of the two molecules are proximal and the N-termini are distal to the dimer interface. The cores of the two domains are essentially identical. The major conformational differences between the two molecules are localized to the dimer interface (Fig. 4). Specifically, the $\beta1$–$\beta2$ loop of RBDb forms part of the interface, whereas the corresponding loop of RBDa is pulled away. Conversely, the C-terminus of RBDa is well ordered at the interface, whereas that of RBDb is disordered beyond residue F132b and does not participate in dimer contacts. These differences appear to result from the breakdown of perfect twofold symmetry due to crystal packing. In the crystal lattice, both RBDa and RBDb are located near a crystallographic screw axis. As a result, both molecules are closely packed against their symmetry mates. Perfect noncrystallographic dyad symmetry would incur steric conflict among symmetry-related molecules and so could not be accommodated by the crystal lattice.

The pseudo-symmetry that relates the two RBDs results in an asymmetric dimer interface. As discussed below, the contacts between RBDa and RBDb centered on P103b and D135a are not recapitulated by the corresponding residues P103a and D135b. However, since the dimer interface is composed of flexible structural elements such as the $\beta1$–$\beta2$ loop, the $\beta7$–$\beta8$ loop, and the C-terminus, it is possible that a symmetric dimer could form in solution, with only minor adjustment of the contact surface.

Intramolecular hydrophobic packing at the dimer interface

In bovine/human RBD, a disulfide bridge is conserved between residue 17 in the $\beta1$–$\beta2$ loop and residue 131/132 in the C-terminus. In rat RBD, however, both C17 and C132 are replaced by phenylalanine residues. The benzene rings of F17a and F132a pack against each other, such that the Cε2 atoms of the two rings are separated by only 3.6 Å (Fig. 5). Their counterparts in RBDb adopt different conformations but are also in contact. Although the surrounding residues adopt different conformations, the phenylalanine pairs in

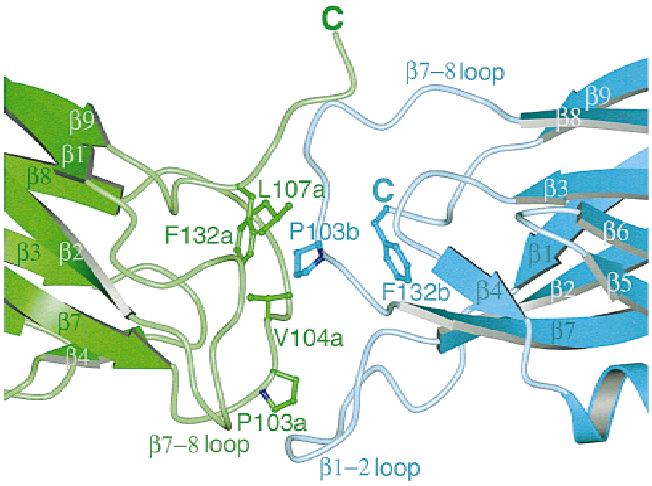

Fig. 4. The asymmetric dimer interface. The orientation is similar to that in Figure 2, and the color scheme used is the same. Residues V104a, L107a P103a,b, and F132a,b are displayed as ball-and-stick models.

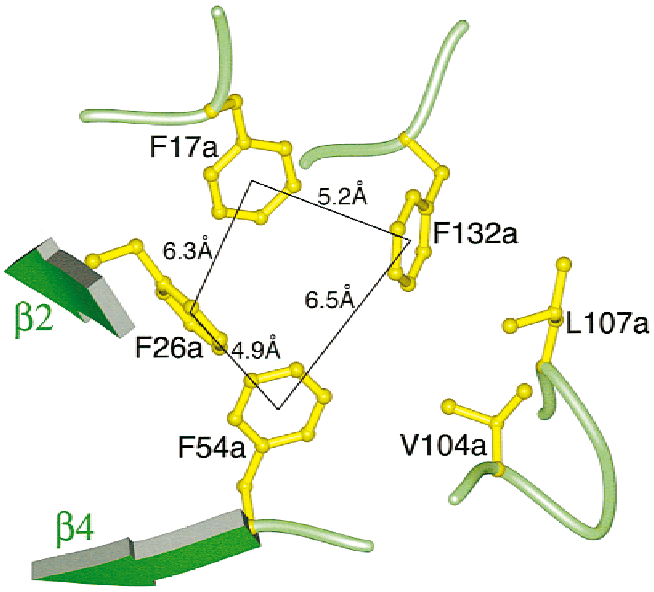

Fig. 5. Aromatic packing interactions in RBDa stabilize the dimer interface. The dimer is rotated approximately 60° about the vertical axis from the view shown in Figure 3A, such that the viewer is looking into RBDa. The trace of the V104a → L107a loop can be used as a reference to orient the viewer. The distances between the benzene ring centroids are shown. The dihedral angle between the ring plane of F17a and that of F132a is 50°; that between F132a and F54a is 60°; F54a and F26a, 70°; F26a and F17a, 80°.

RBDa and RBDb closely overlap the position of the cystine in bovine RBD after superposition of the cores of the three molecules (Fig. 6A). In analogy to the cystine crossbridge in bovine α_2M, and presumably other homologs, the aromatic packing interactions appear to stabilize monomers of rat RBD by bringing their amino- and carboxyl-termini together.

Phenylalanines 17a and 132a form part of an aromatic side-chain network that also includes F26a and F54a (Fig. 5). This network is partially disrupted in RBDb, in part as a consequence of the different conformation adopted by the $\beta1$–$\beta2$ loop (Fig. 2). Packing interactions between phenylalanine residues are the most common of aromatic contacts in proteins (Burley & Petsko, 1985; Singh & Thornton, 1985). The cluster in RBD exhibits the typical edge-to-face "herringbone" packing mode with inter-ring dihedral angles of 50–90° and aromatic ring centroid distances between 4.5 and 7.0 Å (Burley & Petsko, 1985).

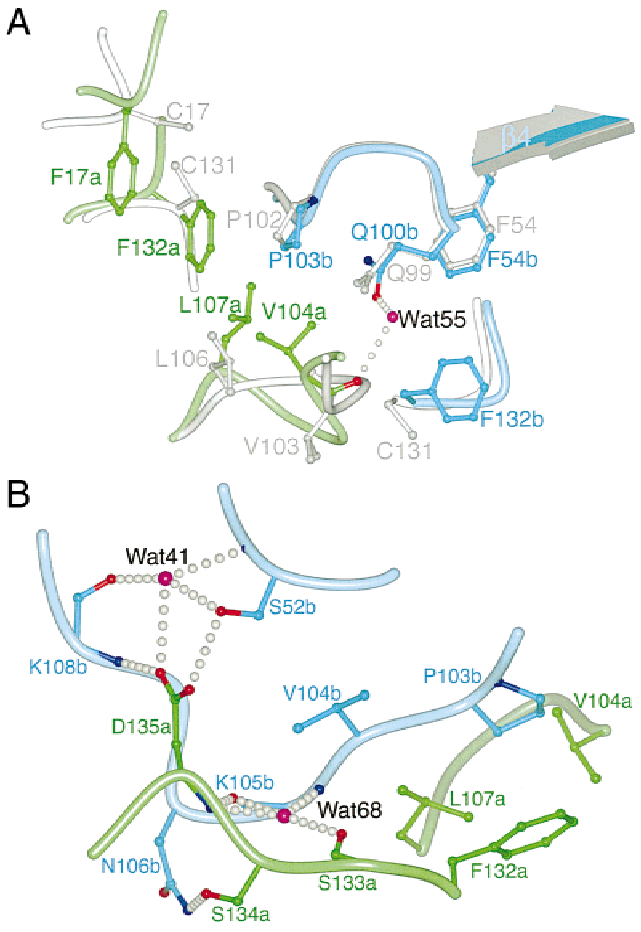

Fig. 6. Details of the dimer interface. **A:** The dimer interface in the neighborhood of residue P103b (cyan). The view is similar to that in Figure 4. Ball-and-stick models of residues are displayed and labeled using the same color code as the backbone ribbon. The structure of the bovine α_2M RBD monomer (gray) is superimposed onto each of the two rat RBD molecules to show the different orientations of side chains that could form or disrupt the dimer. Hydrogen bonds are represented by dotted lines. **B:** The dimer interface about residue D135a that anchors the C-terminus of the RBDa molecule. The dimer is rotated approximately 90° about the horizontal axis toward the reader relative to **A**. The positions of V104a, L107a, F132a, and P103b can be used as a reference for orientation.

The dimer interface

The dimer interface is formed primarily by contacts between the $\beta8$–$\beta9$ loops of the two monomers such that P103b is intercalated between the side chains of L107a and V104a (Figs. 4, 6). The closely packed aromatic amino acids form a nucleus of contacts that may stabilize rat RBD dimers in the crystal and possibly in solution. The F132a : F17a pair connects the dimer interface directly to the aromatic core of RBDa whereas the water-mediated hydrogen bond between V104a and Q100b connects the dimer interface to the core of RBDb. Q100b in turn is in van der Waals contact with the buried F54b (Fig. 6A). The strictly conserved P103b located near the center of the dimer interface is in van der Waals contact with R24a, V104a, L107a, and F132a (Figs. 4, 6). In contrast, the breakdown of dyad symmetry leaves P103a exposed but packed against mainchain atoms of $\beta1$–$\beta2$ loop in RBDb (Fig. 4).

The dimer interface also extends to the peripheral region of the two domains. F132a and D135a form a network of hydrogen bonds, ion pairs and van der Waals interactions that tether the C-terminus of RBDa to the $\beta7$–$\beta8$ loop of RBDb (Fig. 6B). D135a buries the most solvent accessible surface of any residue at the dimer interface (120 Å^2). In total, the dimer interface comprises six hydrogen bonds; 59 and 63% of the contact surface of RBDa and RBDb, respectively, is composed of nonpolar atoms (Jones & Thornton, 1996). The RBDb C-terminus is not discernible near the dimer interface but would be positioned near the $\beta7$–$\beta8$ loop of RBDa.

Equilibrium ultracentrifugation experiments show that rat RBD appears to form a mixture of monomers and dimers at about 50 μM concentration (Fig. 1). In agreement with the above, the buried solvent accessible surface area in the dimer is not very large compared with those of antigen–antibody interfaces (700 Å^2 per monomer vs. ~600 Å^2 per monomer in the RBD dimer) and is in the lower range of surface areas buried in specific oligomeric protein complexes (Janin et al., 1988). Although rat RBD dimers could arise entirely from crystal packing forces, ultracentrifugation and gel filtration experiments show that the ability of rat RBD to dimerize is an inherent property in solution rather than a crystallization artifact. Bovine RBD, though crystallized under conditions similar to those used for rat RBD, fails to form dimers in the crystal lattice (Jenner et al., 1998).

The receptor binding sites on RBD

A prominent feature of the rat RBD dimer is the ridge formed by the two helices of each monomer that are aligned with their axes nearly parallel. The helices are packed in the grooves formed by β-strands 5 and 7, along the edge of the β-sheet (Fig. 2). The protruding $\beta1$–$\beta2$ loop is located on the same edge as the helix and projects outward from the main body of the β-sandwich. As noted above, the $\beta1$–$\beta2$ loops in the two molecules adopt different conformations. Mutagenesis of human RBD indicated that K1370 and K1374 (corresponding to K58 and K62 of rat RBD) are necessary but not sufficient to confer receptor binding activity (Nielsen et al., 1996). Epitope mapping by phage display identified a peptide capable of displacing αM from its receptor. This peptide is composed of residues corresponding to the $\beta1$–$\beta2$ loop (which adopts a helical conformation in bovine and human RBD) and the $\beta2$–$\beta3$ loop at the opposite end of the domain (Birkenmeier et al., 1997). The $\beta1$–$\beta2$ loop, helix 1, and $\beta2$–$\beta3$ loop form three discrete patches arranged progressively further from the dimer interface

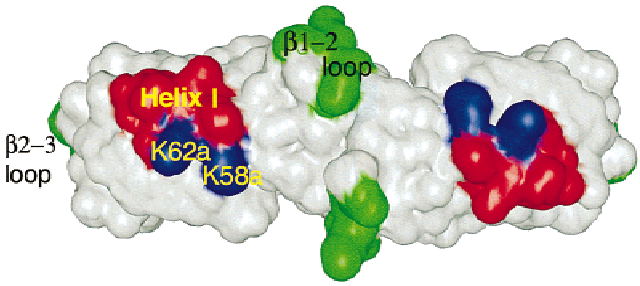

Fig. 7. The solvent accessible surface of the RBD. The view is similar to that in Figure 4. Residues of helix 1 are colored red except for K58 and K62, which are colored blue. Proposed receptor binding residues in β1–β2 or β2–β3 loop are colored green. Residues in RBDa are labeled. Figures were prepared with programs Gl_render (Esser, 1999), GRASP (Nicholls et al., 1991), Bobscript (Esnouf, 1997), Povray (Povray Team, 1998), and Raster3D (Merritt & Bacon, 1997).

(Fig. 7). It is possible that LRP could dock onto the three patches simultaneously when bound to RBD.

The location of the ligand binding site on LRP has not been well defined, but has been proposed to lie within two clusters of cysteine-rich repeats (Neels et al., 1999). Given the small size and highly homologous structures of these repeats, it is possible that multiple RBD binding sites are present on the two clusters, allowing two or more RBD domains to bind simultaneously. An interaction could be envisioned in which translation- or screw-related complement repeats in LRP interact with pairs of dyad-related RBD domains. The exposure of putative receptor binding residues on a contiguous surface of the RBD dimer, or properly oriented monomers, could also induce cross-linking of LRP.

Conclusion

The RBD of rat α_2M appears unusual in its ability to form dimers both in crystals and in solution. There may be significant differences in the mode of dimerization under these two conditions, however. Dimer formation might be favored by the conformational adjustments consequent upon substitution of the cystine cross-bridge present in most RBDs by the pair of phenylalanine residues present in rat α_1M RBD. It is also possible that the RBDs of all αM homologs dimerize after protease or methylamine activation. We have speculated that dimer formation generates an extended receptor binding site that may induce receptor cross-linking or engagement of multiple complement repeats. These conclusions are speculative, however; the real significance of RBD dimerization to the function of rat α_1M must await high resolution structural studies of intact αM, or of RBD in complex with the LRP repeats that comprise its binding site.

Materials and methods

Expression and purification

The cDNA clone encoding the rat α_1-macroglobulin gene was obtained from the American Type Culture Collection (ATCC) and the C-terminal 141 residues representing RBD was amplified by polymerase chain reaction (PCR). Molecular cloning procedures were carried out according to Sambrook et al. (1989) unless stated otherwise. The PCR product was cloned into bacterial expression vector pQE-30 (Qiagen, Hilden, Germany) at Bam HI and Hind III sites. The recombinant vector was transformed into bacterial strain DH5αF′IQ^{TM} (Life Technologies, Rockville, Missouri) to take advantage of the lac I^q repressor gene on the F′ episome, which allows for tight control of RBD expression. Transformed cells were grown in LB medium containing 100 mg/L ampicillin and 25 mg/L kanamycin at 37 °C. Expression was induced with 1 mM isopropyl-1-thiogalactopyranoside (IPTG) at cell optical density $A_{600\,nm}$ of about 0.8. Induction was carried out for 5 h at 37 °C, and the cells were harvested by centrifugation and flash frozen at −80 °C.

Frozen cells were thawed in lysis buffer (50 mM Tris·Cl, pH 8.5, 300 mM NaCl) supplemented with 5 mg/mL lysozyme, 0.5% *n*-octyl-β-D-glucopyranoside, 30 μg/mL DNase I and 20 μg/mL RNase A to promote lysis. The lysis mixture was incubated on ice for 30 min and centrifuged for 1 h at 100,000 *g* and the supernatant was loaded onto a Ni^{2+}-nitrilo-tri-acetic acid (Ni-NTA) column pre-equilibrated with the lysis buffer. The column was washed with lysis buffer followed by lysis buffer plus 5 mM imidazole. The protein was eluted with lysis buffer plus 250 mM imidazole, then dialyzed against loading buffer (50 mM Tris·Cl, pH 7.5, 2 mM dithiothreitol and 1 mM ethylenediaminetetraacetic acid (EDTA)) overnight. The dialysate was subjected to MonoQ anion exchange chromatography (Amersham Pharmacia Biotech, Piscataway, New Jersey). RBD was eluted with a linear gradient of 0 to 1 M NaCl in loading buffer. The yield is about 6 mg/5 g wet cells after MonoQ purification. Fractions containing RBD were concentrated to about 6 mg/mL and aliquoted into 50 μL fractions. The aliquots were flash frozen in liquid nitrogen and stored at −80 °C.

Sedimentation equilibrium ultracentrifugation

Sedimentation equilibrium was performed on a Beckman XL-I Analytical Ultracentrifuge. The initial concentration of rat RBD protein was 1.2 mg/mL in a buffer containing 50 mM Tris·Cl, pH 7.5, 100 mM NaCl, 1 mM EDTA and 1 mM β-mercaptoethanol (BME). One hundred ten microliter protein samples and 130 μL buffer controls were centrifuged at 4 °C using six-sector cells at speeds 18,000 or 20,000 rpm in an An60ti rotor. Absorbance scans were taken at 280 nm with a step size of 0.001 cm; each scan represents the average over 15 replicates. Successive scans were compared graphically using the MicroCal Origin software to ensure that the sample reached sedimentation equilibrium. The partial specific volume of rat RBD was calculated to be 0.732 mL/g by the program SEDNTERP (Hayes DB, Laue T, Philo J, at web site http://home.earthlink.net/~jphilo/SDNUPDAT.exe). Monomer RBD molecular mass was calculated from amino acid sequence to be 17.56 kDa. Data analysis was accomplished with the MicroCal Origin software. Examination of the residuals and minimization of the variance as implemented in the program determined goodness of fit.

Crystallization and data collection

RBD crystals were grown by either hanging or sitting drop vapor diffusion at 20 °C. The first crystals were obtained using Hampton Research Crystal Screen II and the crystallization conditions were optimized. One to two microliters of protein solution were mixed with an equal amount of well solution (22% PEG 6K, 100 mM Na^+·Hepes at pH 7.0, 25 mM $CaCl_2$) on a siliconized glass cover slides and equilibrated against 1 mL of the well solution. Crystals

appeared within one to three days and grew to a maximum size of $1.0 \times 0.03 \times 0.03$ mm in a week. Crystals were enlarged to about 0.06 mm in the second and third dimensions by macroseeding into solutions containing lower precipitant (17.5% PEG 6K as opposed to 22%) and lower protein (3.5 vs. 6 mg/mL) concentrations. Crystals in macroseeded drops appear within one week and continue to grow for one month. Exchanging the $CaCl_2$ with KCl, LiCl, NaCl, or other dication did not increase the size of the crystals. The crystals were harvested in 25% PEG 6K, 50 mM Na^+·Hepes (pH 7.0), 25 mM Tris·Cl (pH 7.5), 135 mM NaCl, 25 mM $CaCl_2$ and 35% glycerol as cryoprotectant, then flash frozen in liquid nitrogen-cooled liquid propane and stored in liquid nitrogen. The crystals belong to space group $P2_1$ with cell constants $a = 64.38$ Å, $b = 36.15$ Å, $c = 77.98$ Å, and $\beta = 105.88$.

A native data set was measured at beam line F-1 of the Cornell High Energy Synchrotron Source (CHESS). Data were recorded on a 2048 binned CCD detector at a wavelength of 0.918 Å under cryogenic temperature (100 K). A total of 182° data were collected in 0.5° oscillation steps using 20 s exposures. Diffraction data were reduced using the HKL software package (Otwinowski, 1993) (Table 1).

Structure solution and refinement

Molecular replacement was performed with the program AMoRe (Navaza, 1994) in the CCP4 suite (CCP4, 1994) using the atomic coordinates of bovine α_2-macroglobulin receptor-binding domain, without modification, as a search model (Jenner et al., 1998). Data from 15 to 3 Å were used for molecular replacement phasing. After rigid body refinement, the top rotation/translation solution gave a correlation coefficient and *R*-factor of 0.55 and 0.48, respectively, whereas those of the next best solution are 0.43 and 0.54. A $2F_o - F_c$ map using the phases derived from molecular replacement clearly revealed the conserved β-strands and difference electron density at sites where the amino acid composition of the search model differs from that of rat α_1M.

Sigma A-weighted $2F_o - F_c$ and $F_o - F_c$ maps were computed for visual inspection and model building. The atomic model was manipulated using the program O version 6.10 (Jones & Kjeldgaard, 1993) and refined using CNS v0.9 (Brünger et al., 1998). Each round of refinement consisted of positional refinement by Powell minimization, individual *B*-factor refinement and simulated annealing slow-cool molecular dynamics, using a maximum likelihood target and monitored by the free *R*-factor. It was evident at the early stage of refinement that several loop regions of the two molecules in the asymmetric unit are significantly different from each other. Therefore, noncrystallographic symmetry restraints were only applied to the secondary structural elements. Refinement using these restraints was monitored by the decrease in the free *R*-factor. Anisotropic *B*-factor and bulk solvent corrections were used throughout the refinement. Stereochemical tests were performed using Procheck (Laskowski et al., 1993) and indicated that 88.6% of the residues fall in the most favorable regions and no residues fall in disallowed regions of the Ramachandran plot (Ramachandran et al., 1963). The coordinates and structure factors have been deposited with RCSB Protein Data Bank (Berman et al., 2000) (accession code 1EDY). Some of the interface analysis was performed with the web site server (http://www.biochem.ucl.ac.uk/bsm/PP/server/) of Jones and Thornton (1996) and others using CCP4 program CONTACT (CCP4, 1994).

Acknowledgments

We thank Lasse Jenner and Jens Nyborg at the University of Aarhus for early access to the coordinates of the bovine RBD structure, John J.G. Tesmer and R. Bryan Sutton for assistance with data collection, Nikki Dossman for characterization and crystallization, David Meyers, Derk D. Binns, and Joseph P. Albanesi for analytical ultracentrifugation analysis, Lothar Esser for assistance with figure preparation, and the staff at CHESS F-1 station for their technical support. This work is supported by Welch grant I1229 to S.R.S. and an American Heart Association Texas Affiliate Grant-in-Aid 966-063 to D.L.D.

References

Andersen GR, Koch TJ, Dolmer K, Sottrup-Jensen J, Nyborg J. 1995. Low resolution X-ray structure of human methylamine-treated α2-macroglobulin. *J Biol Chem 270*:25133–25141.

Armstrong PB, Quigley JP. 1999. Alpha2-macroglobulin: An evolutionarily conserved arm of the innate immune system. *Dev Comp Immunol 23*:375–390.

Berman HM, Westbrook J, Feng Z, Gilliland G, Bhat TN, Weissig H, Shindyalov IN, Bourne PE. 2000. The Protein Data Bank. *Nucleic Acids Res 28*:235–242.

Birkenmeier G, Osman AA, Kopperschlager G, Mothes T. 1997. Epitope mapping by screening of phage display libraries of a monoclonal antibody directed against the receptor binding domain of human alpha2-macroglobulin. *FEBS Lett 416*:193–196.

Blacker D, Wilcox MA, Laird NM, Rodes L, Horvath SM, Go RCP, Perry R, Watson JB, Bassett SS, McInnis MG, et al. 1998. Alpha-2 macroglobulin is genetically associated with Alzheimer disease. *Nat Genet 19*:357–360.

Borth W, Luger TA. 1989. Identification of alpha 2-macroglobulin as a cytokine binding plasma protein. Binding of interleukin-1 beta to "F" alpha 2-macroglobulin. *J Biol Chem 264*:5818–5825.

Brünger AT, Adams PD, Clore GM, Gros P, Grosse-Kunstleve RW, Jiang JS, Kuszewski J, Nilges M, Pannu NS, Read RJ, et al. 1998. Crystallography and NMR system (CNS): A new software suite for macromolecular structure determination. *Acta Crystallogr D54*:905–921.

Burley SK, Petsko GA. 1985. Aromatic-aromatic interaction: A mechanism of protein structure stabilization. *Science 229*:23–28.

CCP4 (Collaborative Computational Project Number 4). 1994. The CCP4 suite: Programs for protein crystallography. *Acta Crystallogr D50*:760–763.

Delain E, Barray M, Tapon-Bretaudiere J, Pochon F, Marynen P, Cassiman JJ, Van den Berghe H, Van Leuven F. 1988. The molecular organization of human alpha 2-macroglobulin. An immunoelectron microscopic study with monoclonal antibodies. *J Biol Chem 263*:2981–2989.

Dolmer K, Huang W, Gettins PGW. 2000. NMR solution structure of complement-like repeat CR3 from the low density lipoprotein receptor-related protein. *J Biol Chem 275*:3264–3269.

Eggertsen G, Hudson G, Shiels B, Reed D, Fey GH. 1991. Sequence of rat alpha 1-macroglobulin, a broad-range proteinase inhibitor from the alpha-macroglobulin-complement family. *Mol Biol Med 8*:287–302.

Esnouf RM. 1997. An extensively modified version of MolScript that includes greatly enhanced coloring capabilities. *J Mol Graph 15*:33–138.

Esser L. 1999. Gl_render version 0.9. http://www.hhmi.swmed.edu/external/Doc/Gl_render/Html/gl_render.html.

Fass D, Blacklow S, Kim PS, Berger JM. 1997. Molecular basis of familial hypercholesterolaemia from structure of LDL receptor module. *Nature 388*:691–693.

Gliemann J, Nykjaer A, Petersen CM, Jorgensen KE, Nielsen M, Andreasen PA, Christensen EI, Lookene A, Olivecrona G, Moestrup SK. 1994. The multiligand alpha 2-macroglobulin receptor/low density lipoprotein receptor-related protein (alpha 2MR/LRP). Binding and endocytosis of fluid phase and membrane-associated ligands. *Ann NY Acad Sci 737*:20–38.

Herz J, Hamann U, Rogne S, Myklebost O, Gausepohl H, Stanley KK. 1988. Surface location and high affinity for calcium of a 500-kd liver membrane protein closely related to the LDL-receptor suggest a physiological role as lipoprotein receptor. *EMBO J 13*:4119–4127.

Holtet TL, Nielsen KL, Etzerodt M, Moestrup SK, Gliemann J, Sottrup-Jensen L, Thogersen HC. 1994. Receptor-binding domain of human alpha 2-macroglobulin. Expression, folding and biochemical characterization of a high-affinity recombinant derivative. *FEBS Lett 344*:242–246.

Huang W, Dolmer K, Gettins PGW. 1999. NMR solution structure of complement-like repeat CR8 from the low density lipoprotein receptor-related protein. *J Biol Chem 274*:14130–14136.

Huang W, Dolmer K, Liao X, Gettins PG. 2000. NMR solution structure of the receptor binding domain of human alpha(2)-macroglobulin. *J Biol Chem 275*:1089–1094.

Hughes SR, Khorkova O, Goyal S, Knaeblein J, Heroux J, Riedel NG, Sahasrabudhe S. 1998. Alpha2-macroglobulin associates with beta-amyloid peptide and prevents fibril formation. *Proc Natl Acad Sci USA 95*:3275–3280.

Janin J, Miller S, Chothia C. 1988. Surface, subunit interfaces and interior of oligomeric proteins. *J Mol Biol 204*:155–164.

Jenner L, Husted L, Thirup S, Sottrup-Jensen L, Nyborg J. 1998. Crystal structure of the receptor-binding domain of alpha 2-macroglobulin. *Structure 6*:595–604.

Jones S, Thornton JM. 1996. Principles of protein-protein interactions. *Proc Natl Acad Sci USA 93*:13–20.

Jones TA, Kjeldgaard M. 1993. *O Version 5.9*. Uppsala, Sweden: Uppsala University. pp 1–161.

Laskowski RA, MacArthur MW, Moss DS, Thornton JM. 1993. PROCHECK: A program to check the stereochemical quality of protein structures. *J Appl Crystallogr 26*:283–291.

Merritt EA, Bacon DJ. 1997. Raster3D: Photorealistic molecular graphics. *Methods Enzymol 277*:505–524.

Moestrup SK, Gliemann J. 1991. Analysis of ligand recognition by the purified alpha 2-macroglobulin receptor (low density lipoprotein receptor-related protein). Evidence that high affinity of alpha 2-macroglobulin-proteinase complex is achieved by binding to adjacent receptors. *J Biol Chem 266*: 14011–14017.

Moestrup SK, Kaltoft K, Sottrup-Jensen L, Gliemann J. 1990. The human alpha 2-macroglobulin receptor contains high affinity calcium binding sites important for receptor conformation and ligand recognition. *J Biol Chem 265*:12623–12628.

Navaza J. 1994. *AMoRe*: An automated package for molecular replacement. *Acta Crystallogr A50*:157–163.

Neels JG, van den Berg BMM, Lookene A, Olivecrona G, Pannekoek H, van Zonneveld A. 1999. The second and fourth clusters of class A cysteine-rich repeats of the low density lipoprotein receptor-related protein share ligand-binding properties. *J Biol Chem 274*:31305–31311.

Nicholls A, Sharp KA, Honig B. 1991. Protein folding and association: Insights from the interfacial and thermodynamic properties of hydrocarbons. *Proteins 11*:218–296.

Nielsen KL, Holtet TL, Etzerodt M, Moestrup SK, Gliemann J, Sottrup-Jensen L, Thogersen HC. 1996. Identification of residues in alpha-macroglobulins important for binding to the alpha2-macroglobulin receptor/Low density lipoprotein receptor-related protein. *J Biol Chem 271*:12909–12912.

Nielsen KL, Sottrup-Jensen L, Fey GH, Thogersen HC. 1995. Expression and refolding of a high-affinity receptor binding domain from rat alpha 1-macroglobulin. *FEBS Lett 373*:296–298.

O'Connor-McCourt MD, Wakefield LM. 1987. Latent transforming growth factor-beta in serum. A specific complex with alpha 2-macroglobulin. *J Biol Chem 262*:14090–14099.

Otwinowski Z. 1993. Oscillation data reduction program. In: Sawyer NIL, Bailey SW, eds. *Data collection and processing*. Daresbury, UK: Science and Engineering Council Daresbury Laboratory. pp 56–62.

Povray Team. 1998. Pov-ray—The persistence of vision ray tracer. http://www.povray.org/.

Ramachandran GN, Ramakrishnan C, Sasisekharan V. 1963. Stereochemistry of polypeptide chain configurations. *J Mol Biol 7*:95–99.

Sambrook J, Fritsch EF, Maniatis T. 1989. *Molecular cloning: A laboratory manual*. Cold Spring Harbor, NY: Cold Spring Harbor Laboratory.

Singh J, Thornton JM. 1985. The interaction between phenylalanine rings in proteins. *FEBS Lett 191*:1–6.

Sottrup-Jensen L. 1987. Alpha2-macroglobulin and related thiol ester plasma proteins. In: Putnam FW, ed. *The plasma proteins*. Orlando, FL: Academic Press. pp 191–291.

Sottrup-Jensen L. 1989. Alpha-macroglobulins: Structure, shape, and mechanism of proteinase complex formation. *J Biol Chem 264*:11539–11542.

Sottrup-Jensen L, Gliemann J, Van Leuven F. 1986. Domain structure of human alpha 2-macroglobulin. Characterization of a receptor-binding domain obtained by digestion with papain. *FEBS Lett 205*:20–24.

Stoops JK, Schroeter JP, Kolodziej SJ, Strickland DK. 1994. Structure-function relationships of human α_2-macroglobulin: Three-dimensional structures of native α_2-macroglobulin and its methylamine and chymotrypsin derivatives. *Ann NY Acad Sci 737*:212–244.

Swenson RP, Howard JB. 1979. Characterization of alkylamine-sensitive site in alpha 2-macroglobulin. *Proc Natl Acad Sci USA 76*:4313–4316.

Warmegard B, Martin N, Johansson S. 1992. cDNA cloning and sequencing of rat alpha 1-macroglobulin. *Biochemistry 31*:2346–2352.

Wilson C, Wardell MR, Weisgraber KH, Mahley RW, Agard DA. 1991. Three-dimensional structure of the LDL receptor-binding domain of human apolipoprotein E. *Science 252*:1817–1822.

Woessner JF. 1991. Matrix metalloproteinases and their inhibitors in connective tissue remodeling. *FASEB J 5*:2145–2154.